scientific reports

Check for updates

OPEN

Mechanistic insights into gut microbe derived siderophores and PHD2 interactions with implications for HIF-1α stabilization

Jainabbi Irshad Ahmed Patel[1], Jagadeesha Poyya[1]✉, Apeksha Padakannaya[1], Namrata Manjunath Kurdekar[1], Ajay Sathayanarayan Khandagale[1], Chandrashekhar Gajanan Joshi[2], Santosh R. Kanade[3] & Kapaettu Satyamoorthy[4]

In oxygen-deprived conditions, cells respond by activating adaptive mechanisms to bolster their survival and protect tissue integrity. A key player in this process is the HIF-1α signaling cascade, meticulously regulated by Prolyl Hydroxylase Domain 2 (PHD2), which orchestrates cellular responses to varying oxygen levels. The primary aim of this investigation is to utilize gut siderophores as inhibitors of PHD2 in ischemic conditions. This study also helps in understanding the structural mechanisms by which gut microbiota regulate HIF-1α via PHD2 inhibition through the secretion of siderophores. We explore potential PHD2 inhibitors through in-silico approaches, specifically molecular docking, binding pose metadynamics, molecular dynamics simulations, and free energy calculations. We evaluated siderophores secreted by gut microbiota as candidate inhibitors for PHD2. Docking studies revealed that Salmochelin SX exhibits the highest binding affinity to PHD2 (− 9.527 kcal/mol), interacting with key residues such as ASP254, TYR310, ASP315, and ARG322. Despite its high affinity, binding pose metadynamics indicated instability for Salmochelin SX, whereas Staphyloferrin A demonstrated superior stability. Molecular dynamics simulations confirmed stable ligand interactions with PHD2, highlighting HIS313 and ASP315 as critical for inhibition. Principal Component Analysis (PCA) and Free Energy Landscape (FEL) analyses underscored conformational changes and binding stability, suggesting that these interactions may stabilize PHD2's active site and have potential therapeutic implications. Additionally, the study reveals how gut microbiota prevent gut dysbiosis through the stabilization of HIF-1α signaling by secreting siderophores.

Keywords Ischemia, Hypoxia, HIF-1α signaling, Gut microbiota, Siderophores

In response to hypoxic microenvironments induced by ischemia, cells activate intricate adaptive pathways to cope with the limited oxygen availability. Among these pathways, the Hypoxia-Inducible Factor-1 alpha (HIF-1) signaling cascade plays a pivotal role in mediating cellular responses to oxygen fluctuations during ischemia[1]. HIF-1 is a transcription factor composed of HIF-1α and HIF-1β subunits, whose stabilization and activation are regulated by Prolyl Hydroxylase Domain 2 (PHD2). Under normoxic conditions, PHD2 hydroxylates HIF-1α, marking it for proteasomal degradation and preventing the formation of the active HIF-1 complex[2]. However, PHD2 activity is reduced under hypoxic conditions leading to HIF-1α stabilization and translocation to the nucleus. Subsequently, HIF-1α dimerizes with HIF-1β, forming the active HIF-1 complex that initiates the transcription of various hypoxia-responsive genes[3].

PHD2 is a crucial enzyme that plays a pivotal role in regulating cellular responses to oxygen levels, a process known as oxygen sensing[4]. PHD2 belongs to the family of prolyl hydroxylases, which are essential components

[1]SDM Research Institute for Biomedical Sciences, Shri Dharmasthala Manjunatheshwara University, Dharwad, Karnataka 580009, India. [2]Department of Biochemistry, Mangalore University, Mangalore, Karnataka 574199, India. [3]Department of Plant Sciences, School of Life Sciences, University of Hyderabad, Hyderabad 500046, Telangana, India. [4]Shri Dharmasthala Manjunatheshwara (SDM) University, Manjushree Nagar, Sattur, Dharwad, Karnataka 580009, India. ✉email: poyyajagadeesha@gmail.com

of cellular oxygen-sensing machinery. These enzymes are key players in the hypoxia-inducible factor (HIF) pathway, a signaling cascade that orchestrates adaptive responses to low oxygen conditions[4,5]. PHD2 specifically targets the HIF transcription factor, facilitating its degradation under normoxic (normal oxygen) conditions by hydroxylating specific proline residues. This hydroxylation marks HIF for recognition by the von Hippel-Lindau (VHL) protein, leading to its subsequent degradation by the ubiquitin–proteasome system[6,7].

The inhibition of PHD2 has emerged as a compelling therapeutic strategy in ischemic diseases characterized by aberrant oxygen sensing and HIF-mediated responses[8]. Interestingly, a number of PHD2 experimental and clinical inhibitors, including vadadustat[9] and Roxadustat[10], have demonstrated promise in stabilizing HIF-1α and triggering adaptive pathways. The effectiveness of these inhibitors in treating diseases like anemia linked to chronic kidney disease and other ischemia disorders is presently being investigated. The liver, lungs, kidneys, intestines, limbs, brain, and heart are among the organs that are impacted by ischemic illness. HIF-1α expression must remain steady during ischemia circumstances. Angiogenesis, glycolysis, erythropoiesis, and cell survival are just a few of the many genes that are among the many downstream targets of HIF-1α. HIF-1α-induced angiogenesis is crucial for promoting the formation of new blood vessels, enhancing oxygen supply to ischemic tissues, and facilitating tissue repair[11,12]. Additionally, HIF-1-driven glycolysis enables cells to adapt their metabolic pathways to generate energy efficiently even in oxygen-deprived conditions, supporting cellular survival[13]. Furthermore, HIF-1α stimulates erythropoiesis through the production of erythropoietin, which increases red blood cell production and improves oxygen-carrying capacity[3,14]. Given the central role of HIF-1 in cellular adaptation to ischemic conditions, the PHD2-HIF-1α axis emerges as a potential therapeutic target[3,15]. Modulating PHD2 activity could stabilize HIF-1α and enhance adaptive cellular responses during ischemia[16].

There are few natural regulators of PHD2, such as low oxygen concentration[17], iron chelator[18], and metabolite from TCA cycle[19]. The regulation of the PHD2 is necessary in a variety of physiological conditions, such as stem cell niche[20] and ischemic[21], where HIF-1α stability is essential to cellular adaptation to low oxygen conditions. Iron chelators have emerged as intriguing agents in the potential inhibition of PHD2[22], primarily due to the role of iron as a crucial cofactor for the enzymatic activity of Prolyl Hydroxylases, including PHD2. These chelators function by sequestering intracellular iron, thereby limiting its availability for PHD2 catalysis. The interaction between iron and PHD2 is pivotal in the hydroxylation of proline residues on hypoxia-inducible factor (HIF), marking it for subsequent degradation under normoxic conditions[18].

PHD2 activity is largely modulated by iron chelators, which are substances that can bind and sequester free iron ions. PHD2's ability to hydroxylate HIF-α is effectively reduced by iron chelators, which decreases the availability of Fe^{2+} at the enzyme's active site. Consequently, this iron-dependent enzyme functions less effectively, stabilizing HIF-α subunits and boosting transcriptional responses mediated by HIF. The HIF pathway, which connects intracellular iron homeostasis with oxygen-sensing systems and their subsequent biological impacts, has been shown to be influenced by both physiological and pharmacological iron chelators. Appreciating the wider interactions between iron metabolism, cellular adaptation to low oxygen, and potential therapeutic approaches that target these pathways requires an understanding of the molecular specifics of how iron chelators interact with and regulate PHD2 activity.

Siderophores are one such iron chelators secreted by microbes. Certain groups siderophores are having capacity to chelates the iron[23]. Siderophores are a fascinating class of small molecules produced by microorganisms, plants, and some fungi to facilitate the acquisition of essential iron from the environment[24]. In the context of PHD2 inhibition, siderophores could sequester extracellular iron, thereby limiting its availability for PHD2 catalysis[25–27].

Additionally, this study elucidates the structural basis of the siderophore regulation of HIF-1α signaling. Studies have shown that gut epithelial barrier integrity is governed by HIF-1α signaling. HIF-1α signaling plays a crucial role in maintaining gut homeostasis by regulating epithelial barrier genes such as *cldn1, jam-a, ocln, muc,* and *itf*[28]. Therefore, stable HIF-1α is essential for maintaining the gut barrier. Some studies have demonstrated that the inhibition of PHD2 in ulcerative colitis can improve outcomes[29,30]. Indeed, PHD2 activity is regulated by gut microbiota in humans through the secretion of siderophore and butyrate (Fig. 1). However, the structural basis of PHD2 regulation by siderophore has not been reported so far. Thus, this study provides insights into how siderophore regulates PHD2 at the structural level and opens up new opportunities for the utilization of siderophore and its analogs for PHD2 inhibition during ischemic conditions.

Our hypothesis revolves around the prospect of harnessing the capabilities of gut siderophores as inhibitors of Prolyl Hydroxylase Domain 2 (PHD2) (Fig. 1) in order to stabilize HIF-1α during ischemic conditions. Also, to understand structural basis of PHD2 & siderophore interactions. Through a comprehensive *in-silico* screening process such as molecular docking, binding pose metadynamics, molecular simulations, trajectory analysis for energy changes, we anticipate the identification and modulation of potential PHD2 inhibitors that can facilitate the preservation of HIF-1α, thereby activating essential adaptive pathways crucial for cellular responses to changes in oxygen levels.

Methodology

Protein preparation

The PHD2 structure with native co-factor Fe^{2+} was retrieved from the Protein Data Bank (PDB ID: 4BQY)[31]. This structure was chosen due to it containing the native co-factor and having a slightly lower resolution (1.40 Å) than other PDB structures in the database. The high angle values of X-ray structure determine a higher quality of the model. The heteroatoms and water molecules were first stripped off the active site, and the structure was optimized to undergo the docking process. To this end, the OPLS3 force field was applied to the protein, and the energy minimized (the lower the energy value, the better). In protein structures, this procedure aids in correcting broken bonds in the arrangement of charge movements and the positions of amides and aromatic groups. The Epik module in Schrödinger was used to ascertain the protonation status of the Fe^{2+} co-factor during

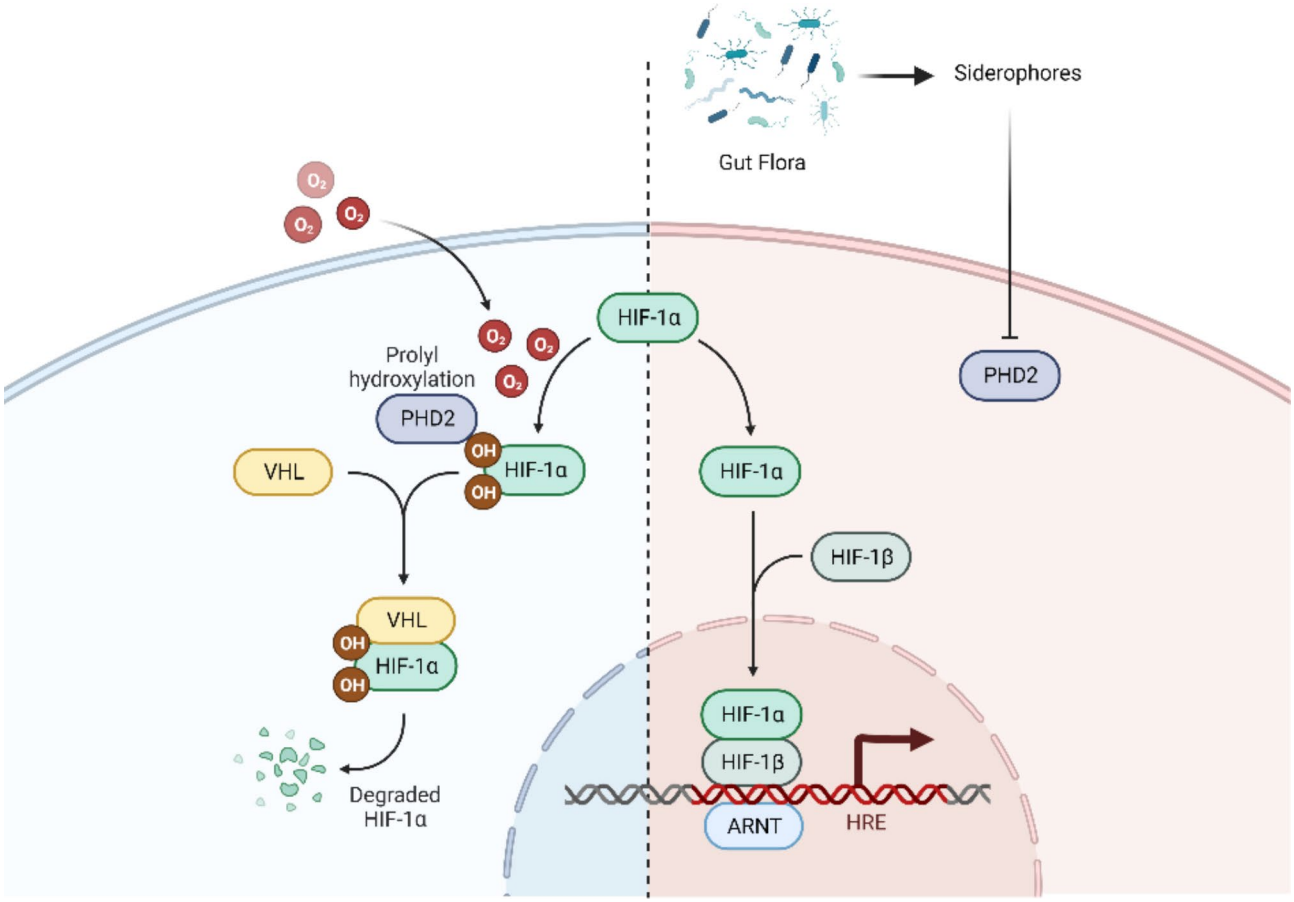

Fig. 1. Illustrates the GUT-PHD2-HIF-1α axis, which is modulated by gut microbial siderophores. Under normoxic conditions, PHD2 hydroxylates the HIF-1α at proline residues at positions 402 and 564. These hydroxylated proline residues are subsequently recognized by VHL and undergo proteasomal-mediated degradation. Given PHD2's role as a non-heme dioxygenase, its catalytic activity relies on iron availability. Notably, a limited number of siderophores secreted by gut microbiota possess the ability to chelate iron, thereby inhibiting PHD2 activity. Consequently, our hypothesis posits that siderophores are equipped to impede PHD2 activity, leading to the activation of the HIF-1α signaling pathway. This activation, in turn, stimulates the expression of genes associated with hypoxia responses.

protein preparation. As a result, Fe^{2+} was accurately described in its biologically relevant state for molecular dynamics and docking simulations. In this study, energy linked to molecular mechanics was determined and steric conflicts in the protein were reduced using the Protein Preparation Wizard and the OPLS3 force field in Schrödinger software[32].

Ligand preparation

Schrodinger's LigPrep module was used to create a library of siderophore and other gut microbial metabolites. The compound was processed with Glide's LigPrep tool[33,34], which generates accurate, and energy minimized 3-dimensional structures and applied sophisticated rules to correct the Lewis structure and eliminates mistakes in the ligand structures. Protonation states of the small molecules were determined using the Epik module integrated within LigPrep, employing a pH range of 7.4 ± 1.0 to approximate physiological conditions. This approach ensures that the compounds are represented in their biologically relevant protonation forms for subsequent docking and molecular dynamics simulations.

Active site and grid generation

The active site was generated using the receptor grid generation module of Schrodinger. The grid enclosed the active site of the PHD2, which includes key factors such as ARG322 and Fe^{2+}. The grid size was about 20X20X20 Å which can accommodate the active site of the protein to allow each ligand to search for the potential binding.

Virtual screening, molecular docking, and MM/GBSA calculations

Protein–ligand docking studies were conducted using the optimized structure of Protein. To evaluate docking efficiency, we employed Molecular Mechanics-Generalized Born Surface Area. (MM/GBSA) study[35–37]. Prime MM/GBSA calculates the binding free energy (*Gbind*) of the siderophores, protein, and complex with Protein

using the MM/GBSA method. Virtual Screening Workflow performs docking of an extensive collection of compounds against one target[38].

Binding pose metadynamics

Binding Pose Metadynamics (BPMD) in Maestro v.2018.4 involves performing 10 independent metadynamics simulations of 10 ns each, using the root-mean-square deviation (RMSD) of ligand heavy atoms as the collective variable (CV). Protein residues within 3 Å of the ligand are selected for alignment prior to RMSD calculation. The system is solvated in a box of SPC/E water molecules, followed by minimization and restrained molecular dynamics (MD) steps to reach 300 K and relieve initial structural strain. A final unbiased MD snapshot of 0.5 ns serves as the reference for the metadynamics production phase.

BPMD evaluates ligand stability using three scores: (1) PoseScore, indicating the average RMSD from the starting pose, where a rapid increase suggests instability. (2) Persistence Score (PersScore), measuring hydrogen bond persistence in the last 2 ns of the simulation, averaged over 10 simulations, with a range from 0 (no or lost interactions) to 1 (fully retained interactions). (3) Composite Score (CompScore), a linear combination of PoseScore and PersScore, calculated as CompScore = PoseScore − 5 × PersScore.

MD simulation & binding free energy calculations

The PHD2 enzyme and four siderophores were simulated. TIP3P, a three-site water model, was used to solvate the system in a cubic box with a 10 Å buffer zone around the enzyme–ligand complex. The system was neutralized by calculating the appropriate number of counterions (Na^+ and Cl^-) to balance the overall charge. Additionally, a fixed salt concentration of 0.15 M was achieved by randomly placing ions in the simulation box via the Desmond system in Schrödinger. This tool adjusts the number of ions on the basis of the system's volume, ensuring that the ionic strength matches physiological conditions. These steps ensured electrostatic neutrality and stability during the simulations. The force field OPLS3e was used to mimic calculations. An isothermal-isobaric (NPT) ensemble was employed, with the pressure and temperature set at 1.01325 bar and 300 K, respectively. A 200 ns simulation time was set, and trajectories were stored every 100 ps. Simulation quality analysis, simulation event analysis, and simulation interaction diagram procedures in the Desmond package were used to analyze the trajectory files. The MD simulations for 200 ns considerably sufficient enough to assess the conformational dynamics and protein–ligand interactions, as indicated by stable RMSD, RMSF, energy profiles, and hydrogen bonding patterns. It would have been mandatory to run the simulation longer if the RMSD of the protein or ligand had a great instability[39].

The binding free energy calculations were performed on the frames obtained from the MD simulation using only the equilibrated part of the MD simulation trajectories. For these calculations, energy components were calculated for each frame after which the frames were clustered and principal component analysis was done to choose the most representative conformations. These analyses gave a snapshot of the structural stability as well as energetics of the PHD2-siderophore complex which conferred dynamic as well as thermodynamic aspects of interaction.

Results

PHD2, also known as prolyl hydroxylase domain 2, plays a crucial role in both normal and disease physiology. In normal physiology, PHD2 is involved in the regulation of cellular responses to oxygen levels, primarily through its interaction with hypoxia-inducible factors (HIFs)[40]. By hydroxylating specific proline residues on HIFs, PHD2 targets them for degradation under normoxic conditions, preventing their accumulation and subsequent activation of hypoxia-responsive genes[2]. This process ensures proper oxygen sensing and adaptation in various tissues and is vital for maintaining homeostasis[41].

Intermolecular interactions are essential in drug discovery as they govern the binding affinity and specificity of drug compounds to their target proteins. These interactions include hydrogen bonding, pi-pi cation, pi-pi stacking, and van der Waals forces of attraction. Hydrogen bonding stabilizes drug-protein complexes, while pi-pi cation and pi-pi stacking interactions contribute to altered pharmacological effects[42]. Van der Waals forces, though weak individually, collectively play a significant role in the overall binding process. Understanding these interactions aids in rational drug design, identifying new drug targets, and predicting pharmacokinetics and safety[43].

Molecular docking studies

To identify suitable lead molecules, docking studies were performed with a natural product library, using Glide to validate the hypothesis. The HIF-1α -binding site of PHD2 contains key residues, including ARG322 and Fe^{2+}, which play an active role in substrate binding through hydrogen bonding interactions. Specifically, the positively charged amino acid ARG322 interacts with PRO564 of the HIF-1α protein within pocket one of PHD2, making it a critical residue in the enzyme's active site and facilitating the interaction with the HIF-1α hydroxylation site, PRO564[44].

A gut metabolite library was screened to identify potential interactions with PHD2, resulting in the discovery of 32 siderophores interacting with PHD2, as detailed in Table S1. Of these, four siderophores were selected for their high affinity for the PHD2 active site. Table 1 presents the binding scores and affinities of compounds Salmochelin SX, Mycobactin, Staphyloferrin A, and Enterobactin towards PHD2. Among these compounds, SALMOCHELIN SX exhibits the highest affinity with a binding score of − 9.527 kcal/mol (MM/GBSA score: − 42.58 kcal/mol). It engages in crucial interactions with the target protein, forming hydrogen bonds with ASP254, TYR310, and ASP315, while accepting hydrogen bonds from TYR303 and ARG322. Additionally, Salmochelin SX coordinates with Fe^{2+}, contributing significantly to its interaction with the key residue ARG322

Compound ID	Docking score (Kcal/mol)	MM/GBSA (Kcal/mol)	Interacting Amino acid residue and cofactor (Fe^{2+})	Interacting Amino Acids residue and co-factors during MD simulation	Amino Acids bridged to Ferrous ion during simulation
Salmochelin SX	−9.527	−42.58	ASP254, TYR303, **TYR310**, ASP315, **ARG322**, Fe^{2+}	**ASP254,** ARG383	HIS313, ASP315, HIS374
Mycobactin	−9.166	−34.25	VAL314, **ARG322**, Fe^{2+}	**ASP254**, THR387	HIS313, ASP315, HIS374
Staphyloferrin A	−7.819	−25.74	**TYR310**, ASP315, **ARG322**, Fe^{2+}	**ASP254**, ARG383, THR387	HIS313, ASP315, HIS374
Enterobactin	−7.302	−38.16	**TYR310, ARG322**	**ASP254**, TYR310, ASP320, TRP389	HIS313, ASP315, HIS374

Table 1. Prioritized compounds list.

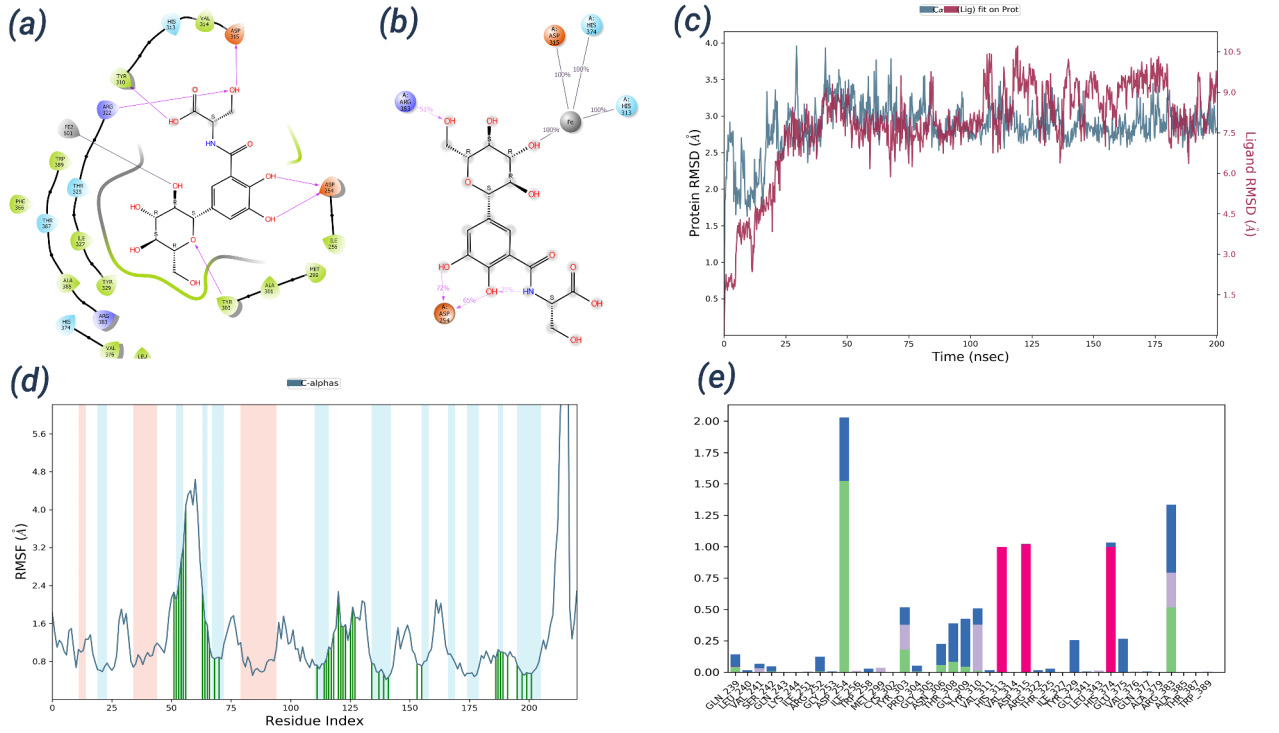

Fig. 2. The Molecular Docking and Dynamic Simulation data for Salmochelin SX and PHD2 complex. (**a**) Docked pose for Enterobactin 1 and PHD2. The key amino acid ARG322, which involves in interactions with HIF-1α being interacts with compound 1 by donating hydrogen bond. (**b**) post MD simulation pose showing changes in active site residue which involved in interaction with PHD2. (**c**) RMSD graph shows the stability of alpha carbon and ligand during simulation period. (**d**) RMSF observed unchanged for protein helix and beta pleated sheets. (**e**) The interaction fraction graph represents the stability of the interaction fraction.

and the co-factor Fe^{2+}. This coordination of Fe^{2+} is vital for stabilizing the ligand–protein complex and plays a pivotal role in determining Salmochelin SX's strong affinity towards PHD2.

Salmochelin SX showed interaction with ASP315, ASP254, TYR303 and ARG322 residue (Fig. 2a). The carboxyl group of compound forms hydrogen bonds with a distance of 1.910 Å with TYR310 respectively. The oxan ring of 3,4,5-trihydroxy-6-(hydroxymethyl) oxan-2-yl] phenyl} formamido) accepts the hydrogen bond from TYR303 (2.178 Å). And the hydroxypropionic group donates hydrogen bond to ASP315 and accepts hydrogen bond from key residue ARG322 with bond distance (2.028 Å) (Fig. S1). The negatively charged ASP254 forms a two-hydrogen bond (1.985 Å and 2.392 Å) with the hydroxyl group of the phenyl ring and Fe^{2+} interaction with the OH group. In the same way, we tested the interactions of other lead molecules.

Next, Mycobactin shows an affinity towards PHD2 with a binding score of − 9.166 kcal/mol. Like Salmochelin SX, it forms multiple interactions with the target protein, donating a hydrogen bond to ARG322 (Fig. 3a) and VAL314 donating and accepting hydrogen bonds from the compound. Furthermore, Mycobactin coordinates with Fe^{2+}, which is crucial for its favorable association with the key residue ARG322 and the co-factor Fe^{2+}. The coordination of Fe^{2+} enhances Mycobactin 's binding to PHD2, contributing to its significant affinity.

The two carboxyl groups of Staphyloferrin A form hydrogen bonds with ASP315 with distances (2.242 Å and 1.480 Å), and one of them accepts a hydrogen bond from key residue ARG322 (2.089 Å). Similarly, at 2.182 Å TYR310 (Fig. 5a) forms an interaction with the hydroxyl group of Staphyloferrin A (Fig. S1). There is also metal coordination with the carboxyl group. Finally, Enterobactin exhibits an affinity towards PHD2 with a binding

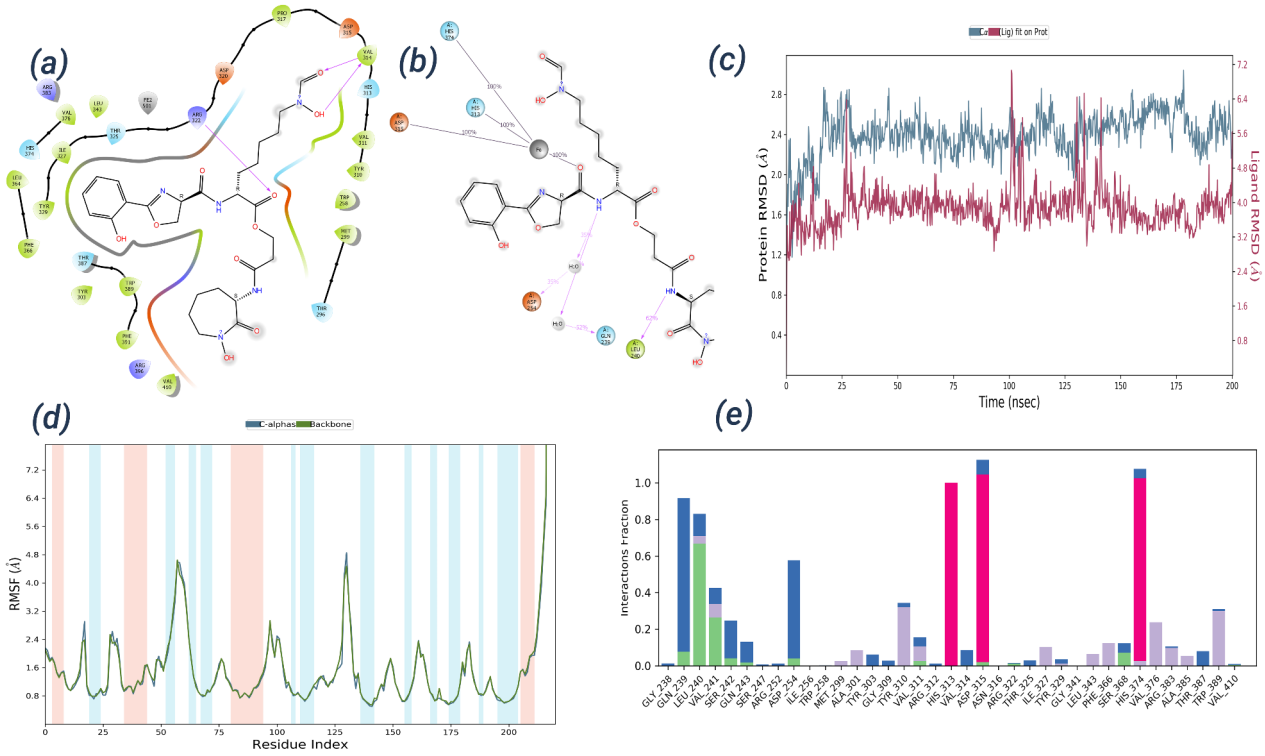

Fig. 3. Illustration of the Molecular Docking and Dynamic Simulation data concerning the complex formed by Mycobactin and PHD2. (**a**) The docked pose reveals the interaction between Mycobactin and PHD2, with the key residues, playing a role in interactions with HIF-1α, forming a hydrogen bond with compound 1. (**b**) The post MD simulation pose highlights alterations in active site residues that engage in interactions with PHD2. (**c**) The RMSD graph depicts the stability of the alpha carbon and ligand throughout the simulation period. (**d**) RMSF indicates the unchanged nature of protein helix and beta pleated sheets. (**e**) The interaction fraction graph illustrates the stability of the interaction fraction.

score of − 7.302 kcal/mol. It forms bonds with the target protein by donating a hydrogen bond (Fig. S1) to TYR310 and engaging in a pi-cation, noncovalent interaction with the key residue ARG322 (Fig. 5a).

The interaction analysis revealed that Salmochelin SX forms a variety of bonds with the target protein, including donating hydrogen bonds to ASP254, TYR310, and ASP315, while accepting hydrogen bonds from TYR303 and ARG322. Moreover, Salmochelin SX coordinates with Fe^{2+}. These intricate bonds are crucial as they play a vital role in the compound's association with the key residue ARG322 and the co-factor Fe^{2+} within PHD2's active site. This strong and specific binding can modulate PHD2's enzymatic activity, potentially leading to therapeutic effects in the context of diseases associated with oxygen sensing and HIF regulation. Comparing the results to the Salmochelin SX, Aerobactin, Staphyloferrin A, and Enterobactin also exhibited significant affinities towards PHD2, albeit with slightly lower binding scores compared to Salmochelin SX. Mycobactin, like Salmochelin SX, forms multiple hydrogen bonds with the target protein (Fig. 3a), while Staphyloferrin A and Enterobactin donate hydrogen bonds (Figs. 4a and 5a) and engage in pi-cation, non-covalent interactions, respectively, with key residue ARG322.

Binding pose metadynamics analysis

The Binding Pose Metadynamics (BPMD) analysis was performed on four siderophores such as Enterobactin, Staphyloferrin A, Mycobactin, and Salmochelin SX complex with PHD2 assessing their binding stability. The BPMD metrics utilized, including PoseScore, PersScore, and CV RMSD, provided detailed insights into the stability and persistence of ligand binding interactions.

The collective variable RMSD (CV RMSD) values over a 10 ns metadynamics simulation provide additional insights into ligand stability. CV RMSD measures the deviation of the ligand's collective variables (such as dihedral angles and specific atomic distances) relative to their initial states, offering a detailed view of the ligand's conformational changes during the simulation. Enterobactin's CV RMSD steadily increased to about 1.5 Å, indicating moderate fluctuations and instability. Staphyloferrin A's CV RMSD increased to around 1.7 Å, supporting its position as the most stable ligand among those analyzed. Mycobactin's CV RMSD rose rapidly to approximately 3.5 Å, confirming significant instability. Salmochelin SX showed the most rapid CV RMSD increase, reaching about 3.6 Å, corroborating its high PoseScore and indicating the greatest instability (Fig. 6a).

Further, PoseScore measures the average RMSD of the ligand heavy atoms relative to the initial coordinates, serving as a crucial indicator of binding pose stability. A rapid increase in PoseScore suggests that the ligand is

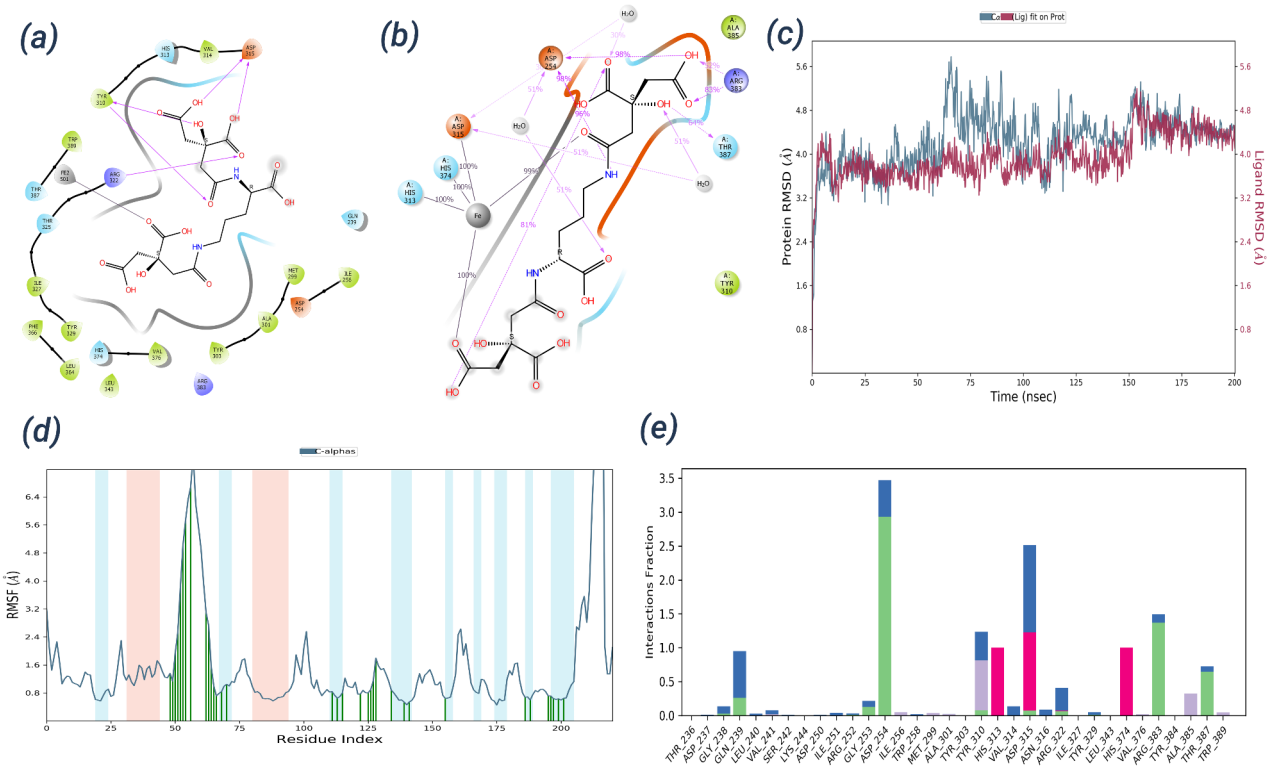

Fig. 4. The molecular docking and dynamic simulation results showing affinity of Staphyloferrin A with PHD2. Staphyloferrin A and PHD2 engage as shown by the docked pose (**a**), with Staphyloferrin A and the important amino acids form bonds during docking studies. Changes in active site residues that interact with PHD2 are highlighted in the post MD simulation pose (**b**). (**c**) The alpha carbon and ligand stability during the course of the simulation is shown by the RMSD graph. The protein helix and beta pleated sheets remain intact, as indicated by (**d**) RMSF. (**e**) An illustration of the interaction fraction's stability is provided by the graph.

not in a well-defined energy minimum, potentially indicating inaccurate modeling. Enterobactin exhibited a PoseScore of 2.89, indicating moderate instability. Staphyloferrin A had a PoseScore of 2.26, suggesting relatively better stability. Mycobactin's PoseScore of 3.69 revealed significant instability, while Salmochelin SX, with a PoseScore of 3.51, also indicated high instability (Fig. 6b). These scores suggest that Staphyloferrin A had the most stable binding pose among the four siderophores, whereas Mycobactin and Salmochelin SX were the least stable.

The PersScore measures the persistence of hydrogen bonds between the ligand and protein residues throughout the simulation. It is calculated as the fraction of frames in the last 2 ns of the simulation that have the same hydrogen bonds as the input structure, averaging over all 10 repeat simulations. Enterobactin had a very low PersScore of 0.04, indicating minimal hydrogen bond persistence. Staphyloferrin A's PersScore of 0.33 suggested more persistent hydrogen bonding, contributing to its relative stability. Mycobactin, with a PersScore of 0.77, showed the highest hydrogen bond persistence among the ligands, despite its overall instability indicated by the PoseScore. Salmochelin SX had a PersScore of 0.00, signifying a complete lack of persistent hydrogen bonds, which correlates with its high PoseScore and overall instability (Fig. 6b).

The Composite Score (CompScore) is a linear combination of PoseScore and PersScore, calculated as CompScore = PoseScore − 5 × PersScore. This score integrates both the geometric stability and interaction persistence of the ligands. Enterobactin had a CompScore of 2.69, indicating moderate overall stability. Staphyloferrin A had a CompScore of 0.61, suggesting the best overall stability among the ligands. Mycobactin's CompScore of -0.16, despite a high PoseScore, reflects the influence of its persistent hydrogen bonds. Salmochelin SX's CompScore of 3.51 further confirms its high instability.

The BPMD results highlight significant variability in the stability of the siderophore binding poses within the pHD2 protein. Staphyloferrin A demonstrated the most favorable stability profile with a low PoseScore, moderate PersScore, and the best CompScore, indicating it could be a promising candidate for further studies in drug design due to its stable and persistent binding interactions. Enterobactin, while showing moderate stability, had minimal hydrogen bond persistence, suggesting it may not form sufficiently stable interactions for therapeutic applications. Mycobactin, despite having the highest PersScore, displayed significant overall instability, indicating that its persistent hydrogen bonds were not sufficient to ensure a stable binding pose.

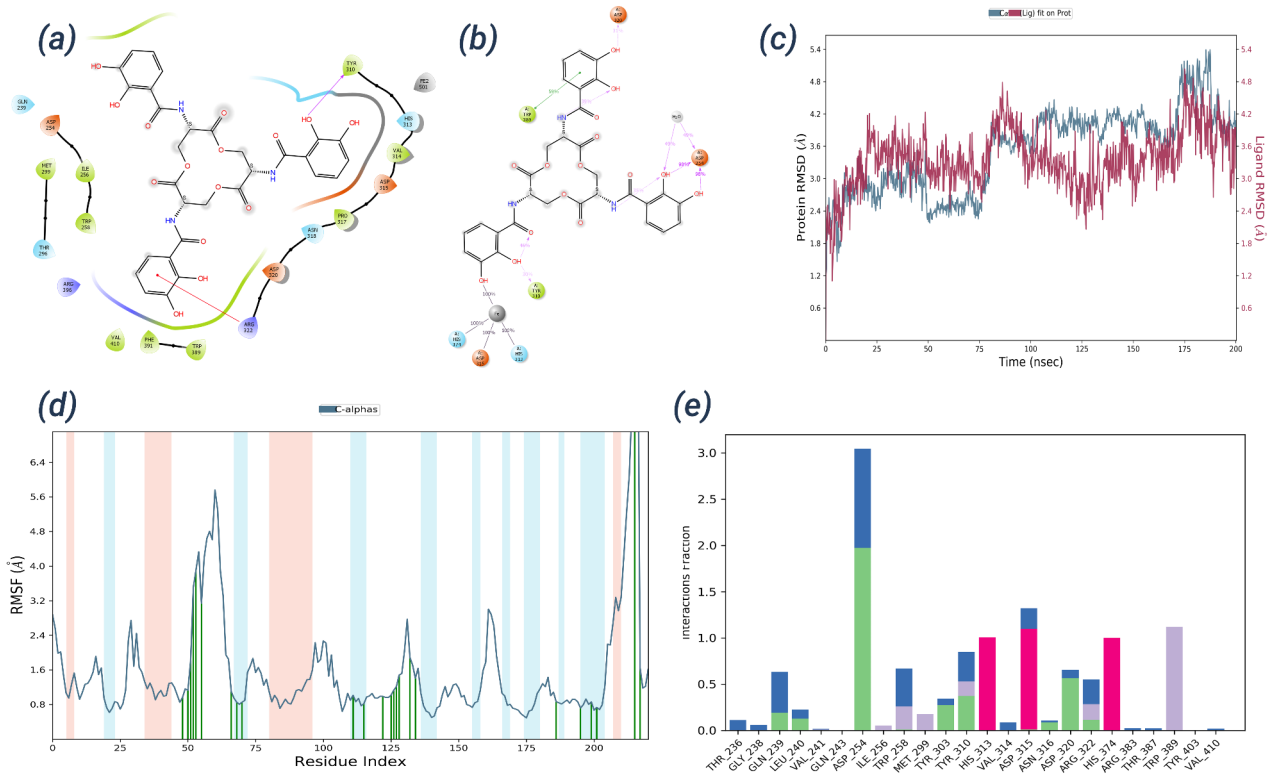

Fig. 5. The complex formed by Enterobactin and PHD2, along with the outcomes of molecular docking and dynamic simulation. As indicated by the docked position (**a**), Enterobactin interacts with PHD2. In the post MD simulation pose (**b**), changes in active site residues that interact with PHD2 are noted. (**c**) The RMSD graph displays the stability of the ligand and alpha carbon throughout the simulation. (**d**) RMSF shows that the beta pleated sheets and protein helix are still intact. (**e**) The graph presents a picture of the stability of the interaction fraction.

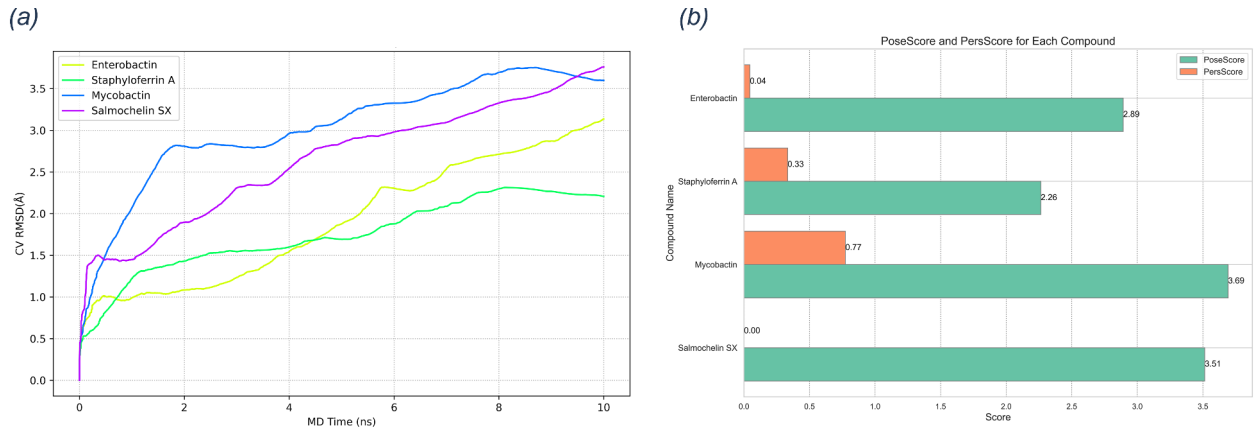

Fig. 6. The Binding Pose Metadynamic Analysis. (**a**) Plot of simulation duration versus average RMSD estimate for siderophores and PHD2. (**b**) Plot showing PoseScore and PersScore for each complex of siderophore & PHD2.

Salmochelin SX, with both high PoseScore and zero PersScore, was the least stable, suggesting it may not be a viable candidate for lead development.

Molecular dynamic simulation

The MD simulations for 200 ns are sufficient to assess conformational dynamics and protein–ligand interactions, as indicated by stable RMSD, RMSF, energy profiles, and hydrogen bonding patterns. It would have been mandatory to run the simulation longer if the RMSD of the protein or ligand had a great instability.

The MD simulation revealed stable conformational changes in the target proteins upon ligand binding (Fig. 2b, c). During the MD simulation of Salmochelin SX and PHD2 complex, the RMSD of alpha carbon and Salmochelin SX initially fluctuated but stabilized after 30 ns, with a final RMSD change of less than 3 Å. The Root Mean Square Fluctuation (RMSF) of the protein–ligand complex showed fluctuations only in the loop regions, a common occurrence during MD simulations (Fig. 2d). Ligand contact had no significant impact on protein RMSF, even in the beta pleated sheets.

The simulation interaction graph represented the strength of bonded interactions, with 40 bonds observed. Only a few bonds, like ASP254, HIS313, ASP315, HIS374, and ARG383 (Fig. 2e), remained in contact for more than 30% of the simulation time. ASP254 had the highest interaction, forming hydrogen bonds and water bridges, while ARG383 had similar interactions. The PHD2 enzyme's co-factor, Fe^{2+}, interacted with histidine and aspartate, specifically HIS313, ASP315, and HIS374 (Fig. 2a, b). This interaction was not present during molecular docking but formed during MD simulations. This interaction is crucial for inhibiting PHD2, as the ferrous ion plays a pivotal role in oxygen-mediated oxidoreductase reactions.

Mycobactin displayed similar results to the Salmochelin SX, with changed interactions (Fig. 3b) compared to its docking results (Fig. 3a) with RMSD values for the alpha carbon and ligands staying below 3 Å (Fig. 3c). During the simulation, RMSF for the protein primarily fluctuated in the loop regions, as is typically observed in loop regions (Fig. 3d). Ligand interactions with the protein did not induce significant fluctuations. The Ligand contact graph, showing interaction fractions, revealed numerous interactions (Fig. 3e). Some of these interactions persisted with the protein for over 30% of the simulation time. In the two-dimensional pose view, ASP254, TYR310, and ARG383 formed hydrogen bonds with the protein–ligand, which had the highest interaction fraction scores (Fig. 3e). The ferrous ion's connection with HIS313, ASP315, and HIS374 played a substantial role in the ligand interaction (Fig. 3b). These ionic interactions were nearly as significant as hydrogen bonding in terms of interaction strength. This interaction is crucial, and inhibiting the ferrous ion may reduce PHD2 enzyme activity. Furthermore, a few water bridges formed during the simulation, involving THR236 and THR387. The few interactions found during the docking studies were missing and additional interactions were observed. This may be due to the structural changes undergoes during MD simulation.

Further, Staphyloferrin A and Enterobactin have similar results like Salmochelin SX and Mycobactin in the case of protein and ligand RMSD (Figs. 4 and 5c) and RMSF (Figs. 4 and 5d). The post MD simulation interaction pose (Figs. 4b and 5b) showed changes in interaction compared to docking pose (Figs. 4a and 5a). RMSF results both siderophores (Staphyloferrin A and Enterobactin) was found changes in only loop regions of the PHD2 (Figs. 4d and 5d). In Staphyloferrin A and PHD2 complex, ARG254, ARG383, and THR387 were formed hydrogen bonds (Fig. 4e). Ferrous ion showed the same interaction with Staphyloferrin A (Fig. 4b) as Salmochelin SX and Mycobactin. In this case water bridge observed with ASP254 and ASP325 (Fig. 4b and e). Enterobactin was found stable throughout the simulations. The interaction of residues was changed during simulation compared to docked pose (Fig. 5b). Further, RMSD (Fig. 5c), RMSF (Fig. 5d) were found stable and there are no changes observed. Enterobactin showed ASP254, TYR310, ASP320 hydrogen bonded (Fig. 5b, e) to the protein for more than 30% of simulation time and TYR389 showed pi-pi cationic interaction.

The Root Mean Square Deviation (RMSD) is used to determine the average change in displacement of a group of atoms in relation to a reference frame. It is useful for assessing the structural conformation of a protein during a simulation. By monitoring the RMSD, one can gain insights into the protein's stability and whether it has reached equilibrium. Additionally, the ligand RMSD, which is displayed on the right-axis, can provide information on the stability of the ligand with respect to the protein and its binding pocket.

The final RMSD changes for both proteins and ligands in all simulations (Salmochelin SX, Mycobactin, Staphyloferrin A, and Enterobactin) remained below 3 Å (Figs. 2c, 3c, 4c, and 5c). While initial fluctuations are common, stabilization after 30 ns suggests a well-equilibrated system (Fig. 2c). Notably, changes of 1–3 Å are acceptable for small, globular proteins like those studied here. Larger deviations would suggest significant structural rearrangements, which we did not observe.

The RMSF analysis provided valuable insights into the local protein dynamics and the impact of ligand binding on these motions (Figs. 2d, 3d, 4d, and 5d). It quantifies the average fluctuation of individual protein residues compared to a reference structure. Peaks in the RMSF plots were primarily confined to the loop regions of the proteins in all simulations (Salmochelin SX, Mycobactin, Staphyloferrin A, and Enterobactin). This is a well-established observation in MD simulations, as loop regions inherently possess greater flexibility compared to secondary structures like alpha helices and beta pleated sheets. Notably, ligand binding did not significantly alter the overall protein dynamics. Even in the structurally rigid beta pleated sheet regions, the RMSF values remained unaffected by ligand presence (Fig. 2d). The consistent pattern of loop region fluctuations and minimal ligand impact on protein dynamics reinforces the notion that ligand binding, while crucial for function, does not necessarily translate to global protein destabilization.

The protein–ligand interactions for Salmochelin SX, Mycobactin, Staphyloferrin A, and Enterobactin complexes with the PHD2 protein (Figs. 2e, 3e, 4e, and 5e) can be categorized into four main types: hydrogen bonds, hydrophobic interactions, ionic interactions, and water bridges. There was a number of key residues that maintained contact with the ligand for a significant portion of the simulation time (> 30%). These residues play a crucial role in ligand binding and function. A notable observation is the interaction of the PHD2 enzyme's co-

factor, Fe^{2+}, with specific histidine and aspartate residues (HIS313, ASP315, and HIS374). The importance of this interaction lies in the crucial role Fe^{2+} plays in the oxygen-mediated oxidoreductase activity of PHD2. Disrupting this interaction through ligand binding likely contributes to PHD2 inhibition. These findings demonstrate the valuable insights gained from MD simulations compared to static docking approaches.

The equilibration process of molecular dynamics (MD) simulations is described in the supplementary material in the form of Fig. S2–S5. In the case of Salmochelin SX (Fig. S2), the system has maintained constant Rg, SASA, and MSA suggestive of compact conformations and conformational stability of interacting residues with tiny RMSF acquires for the ligand. Fig. S3 Mycobactin had stable compact conformations of proteins and fluctuations of protein surfaces, indicating that RMSF represented ligand stability. Staphyloferrin A showed structural and surface interaction values in complete accordance, as well as almost rigid behavior shown by the ligand (Fig. S4). Enterobactin (Fig. S5) kept the protein compactness and interaction characteristics nearly constant, the RMSF data supported the ligand stability for the entire simulation.

In a molecular dynamic simulation, we studied four compounds interacting with the PHD2 protein. These simulations showed that the protein and compounds changed their shapes but eventually stabilized. The compounds interacted with the protein without causing major fluctuations. We found specific interactions, like hydrogen bonds, that were crucial for inhibiting PHD2. These results differed from initial predictions using molecular docking, highlighting the importance of dynamic simulations in understanding how drugs interact with proteins.

Free energy landscape of PHD2- siderophore interaction

The PCA was performed to identify the essential dynamics and significant conformational changes in the protein upon ligand binding. The free energy landscapes (FELs) were then generated by projecting the MD trajectories onto the first two principal components, revealing the conformational space sampled by the PHD2 enzyme in the presence of each siderophores.

For Salmochelin SX, the FEL (Fig. 7a) displayed two major energy minima, indicating two dominant conformational states. The depth of these energy wells suggested that Salmochelin SX induces stable binding modes within the PHD2 enzyme. Mycobactin, however, showed a broader energy distribution with multiple minima in its FEL (Fig. 7b), indicating a higher degree of conformational flexibility and a diverse range of binding poses.

The FEL for Staphyloferrin A (Fig. 7c) revealed three distinct energy minima, with relatively shallower wells compared to Salmochelin SX, indicating moderate stability in binding interactions. Lastly, Enterobactin's FEL (Fig. 7d) was similar to that of Salmochelin SX, with two significant energy minima, suggesting that Enterobactin also stabilizes specific conformations of the PHD2 enzyme, potentially contributing to its binding efficacy.

Cross-correlation analysis was performed to examine the correlated motions within the protein, with the results illustrated in Fig. 8. The cross-correlation matrix for Salmochelin SX (Fig. 8a) showed high correlation in the binding region, indicating coordinated movements that may stabilize the binding site. For Mycobactin (Fig. 8b), diverse correlation patterns were observed, reflecting a range of dynamic interactions. Staphyloferrin A (Fig. 8c) exhibited moderate correlation in specific regions, indicating intermediate binding stability, while Enterobactin (Fig. 8d) showed strong correlated motions similar to Salmochelin SX, supporting its binding efficacy.

The PCA and FEL analyses provided significant insights into the conformational dynamics and binding interactions of the PHD2 enzyme with different compounds. The results indicated that Compounds A and D have strong and specific binding interactions, as evidenced by their well-defined energy minima and high correlation in the binding regions. These findings suggest that these compounds effectively stabilize specific conformations of the PHD2 enzyme, potentially enhancing their inhibitory effects.

In contrast, Mycobactin exhibited a higher degree of flexibility and diverse binding poses, as reflected in its broader energy distribution and varied correlation patterns. This flexibility might confer an advantage in binding to different conformational states of PHD2, but it might also lead to lower specificity and efficacy. Staphyloferrin A demonstrated moderate stability, with distinct conformational states and intermediate correlation patterns, indicating that it has a balanced interaction with the PHD2 enzyme.

Discussion

Human organs undergo various physiological conditions such as ischemia, where flow of blood is reduced and subsequently lacks oxygen supply to tissues or organs[45,46]. In this context, this study was conducted to identify potential inhibitors of PHD2, an enzyme involved in the regulation of Hypoxia-Inducible Factor (HIF), could be a potential strategy to mitigate the effects of ischemia[47,48]. HIF is a transcription factor that plays a key role in cellular responses to low oxygen levels, and its stabilization can promote cellular adaptation and survival under hypoxic conditions[11].

An *in-silico* analysis of selected gut microbial siderophores was done to screen and identify molecules that may have the ability to inhibit PHD2. Results showed that, among 103 molecules, four lead molecules had interactions with key residues. First, Salmochelin SX exhibits the highest affinity with a binding score of − 9.527 kcal/mol. It engages in crucial interactions with the target protein, forming hydrogen bonds with ASP254, TYR310, and ASP315, while accepting hydrogen bonds from TYR303 and ARG322. Additionally, Salmochelin SX coordinates with Fe^{2+}, contributing significantly to its interaction with the key residue ARG322 and the co-factor Fe^{2+}. This coordination of Fe^{2+} is vital for stabilizing the ligand–protein complex and plays a pivotal role in determining Salmochelin SX's strong affinity towards PHD2.

Salmochelin SX, secreted by *Salmonella enterica* characterized as a catecholate-type siderophore[49], exhibits promising attributes that may contribute to mitigating oxidative stress during ischemic reperfusion. In the intricate milieu of cellular responses to oxidative challenges, particularly in the context of the Fenton reaction

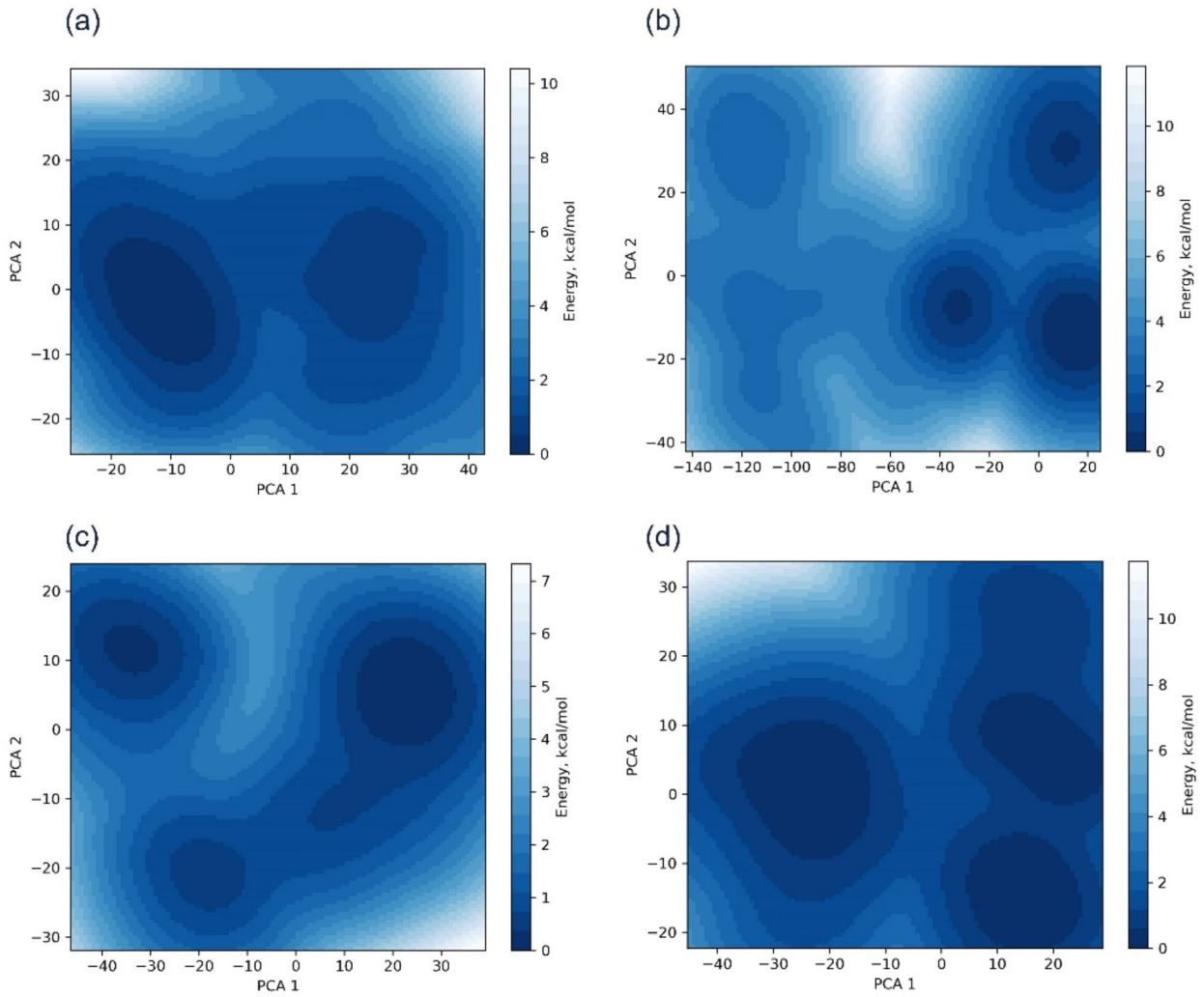

Fig. 7. Free energy landscapes along PCA1 and PCA2 for (**a**) Salmochelin SX, (**b**) Mycobactin, (**c**) Staphyloferrin A, and (**d**) Enterobactin complex with PHD2.

where hydrogen peroxide (H2O2) interacts with intracellular iron sulfur clusters, leading to the generation of harmful free radicals like hydroxyl radicals, Salmochelin SX emerges as a potential protective agent[50].

During ischemic reperfusion, when tissues experience a restoration of blood flow, the potential for reactive oxygen species (ROS) generation is heightened[46]. Salmochelin SX, with its catecholate nature, could play a pivotal role in reducing ROS production. Recent findings have highlighted the capacity of catecholate siderophores, including Salmochelin SX, to act as defenders against oxidative stress, offering a positive perspective on its potential applications. Even though, Salmochelin SX part of a pathogenic microbial strain, it may have therapeutic application where proper balance of gut microbiota can regulate the level of the pathogenicity of the certain bacterial strains[51,52].

The catecholate-type siderophore Enterobactin, previously examined for its anticancer properties, showcased cytotoxic effects on two monocyte tumor cells while leaving bone marrow–derived macrophages unharmed in a study by Saha et al.[53]. The investigation unveiled a significant increase in the intracellular labile iron pool in both cell lines, indicative of a disruption in iron homeostasis induced by the siderophore. Additionally, Enterobactin demonstrated a dose-dependent inhibition of the generation of reactive oxygen species (ROS) by mitochondria. These combined effects, involving alterations in iron levels and the attenuation of ROS production, have the potential to induce apoptosis in cancer cells[53].

Mycobacterium smegmatis produces the mycobactin, which has strong antiproliferative action against leukemia, breast, and liver cancer cell lines[54]. Mycobactin showed interaction with TYR310, ASP254, ARG322, ASN318 residues. The hydroxyl group of compound accepts hydrogen bond from TYR310 with bond distance (2.010 Å) and simultaneously it donates hydrogen bond to ASP254. The carbonyl group of compound forms hydrogen bond interaction with ASN318 (2.031 Å) and carboxyl group of Mycobactin accepts hydrogen bond from key residue ARG322 with a bond distance of 2.037 Å. It also forms metal coordination Fe^{2+} with carboxyl

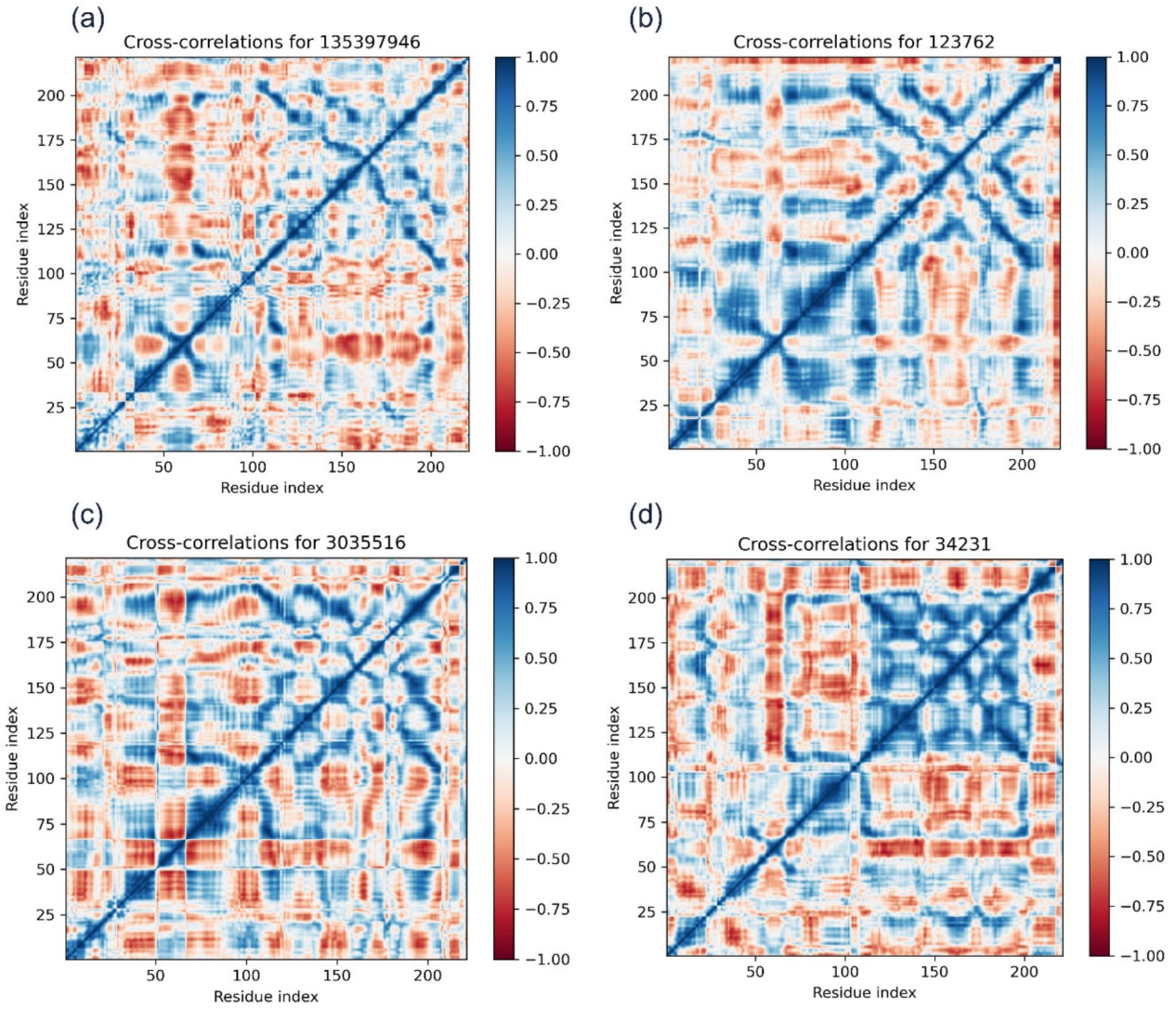

Fig. 8. Cross-correlation maps of residue motions for (**a**) Salmochelin SX, (**b**) Mycobactin, (**c**) Staphyloferrin A, and (**d**) Enterobactin complexes with PHD2.

and hydroxyl groups. Similarly, Staphyloferrin A demonstrates an affinity towards PHD2 with a binding score of -7.819 kcal/mol. It establishes bonds with the target protein, donating a hydrogen bond to TYR310 and ASP315, while accepting hydrogen bonds from TYR310 and ARG322. Like Salmochelin SX and Mycobactin, Staphyloferrin A also coordinates with Fe^{2+}, and this coordination significantly influences its interaction with the key residue ARG322 and the co-factor Fe^{2+}. The coordination with Fe^{2+} is a critical determinant in Staphyloferrin A's affinity towards PHD2. Similar to the other compounds, Enterobactin also coordinates with Fe^{2+}, contributing significantly to its interaction with ARG322 and Fe^{2+}. The coordination of Fe^{2+} plays a vital role in stabilizing Enterobactin 's binding to PHD2. In Enterobactin, the hydroxyl group of the benzene ring forms a hydrogen bond interaction with TYR310, with a bond distance of 1.699 Å. It also has a Pi-cation interaction, i.e., a noncovalent bond with key residue ARG322. In this study, ARG322 most often interacts with the carboxyl group of lead molecules. This kind of observation in reported studies, where small molecules are able to inhibit the activity of PHD2[44].

The coordination of Fe^{2+} is crucial for the interactions between lead compounds and PHD2, significantly impacting their binding with the key residue ARG322 and the co-factor Fe^{2+}. These interactions are essential for stabilizing the ligand–protein complexes and influencing the compounds' overall affinities towards PHD2. Fe^{2+} coordination also plays a pivotal role in regulating PHD2's enzymatic activity[55] and is important in the oxygen-sensing pathway[25]. In addition to the interactions, the BPMD metrics, Staphyloferrin A is identified as the most stable and potentially effective ligand for binding to PHD2. Its low PoseScore, moderate PersScore, and favorable CompScore indicate that it maintains a well-defined binding pose with persistent interactions, making it a strong candidate for drug design. The other ligands, while showing some favorable characteristics, do not achieve the

same level of stability and interaction persistence as Staphyloferrin A. Enterobactin, despite having a moderate PoseScore, suffers from low PersScore, reducing its potential effectiveness. Mycobactin, with its high PersScore, still exhibits significant instability overall. Salmochelin SX, with the highest instability across all metrics, is the least viable candidate.

The MD simulation study indicates changes in binding pose, which substantiates the BPMD. Further, to understand free energy changes during MDS, we did PCA analysis of trajectory. The cross-correlation analysis further supported these observations by highlighting the coordinated motions within the protein, particularly in the binding regions of Salmochelin SX and Enterobactin. These coordinated movements are likely critical for stabilizing the binding interactions and enhancing the compounds' inhibitory potency. In the cross-correlation matrices, the strong correlations observed for Salmochelin SX and Enterobactin reinforce the idea that these compounds induce specific, stabilizing interactions within the PHD2 enzyme. For Mycobactin, the varied correlation patterns suggest a more dynamic and flexible interaction, while Staphyloferrin A's moderate correlations indicate intermediate stability and binding efficacy.

During MD, the changes in ligand RMSD are a result of the ligand's conformational changes within the binding pocket rather than escaping. We observed that the RMSD of the protein differs during different protein–ligand complex MD simulations. This variation is attributed mainly to the different structures of the ligands. The specific structure of each ligand affects how it interacts with the proteins.

This work helps in understanding the regulation of PHD2 by gut siderophores by means of the proposed mechanisms, which are based on molecular dynamics simulations, docking studies, and free energy prediction. Nonetheless, the computational methods used in the current work provide a solid framework upon which molecular interactions and hypotheses can be investigated; however, more experimental work in the future would be a logical and necessary direction.

Additionally, the analysis involving the MM/GBSA-based binding free energy calculations and binding site metadynamics conducted in this work, along with trajectory analyses, provides a thorough picture of the thermodynamics of PHD2 inhibition. These enhanced computations are adequate to provide the molecular and energy dependence needed for the postulated mechanisms and are very useful for analyzing protein–ligand interactions.

This study provides a comprehensive understanding of how gut-derived siderophores interact with PHD2, revealing the molecular basis of HIF-1α signaling regulation. Our analysis demonstrates the stability of these interactions, the dynamics of the protein–ligand complexes, and the overall energy of the system. This study bridges the gap in understanding how gut microbiota influence HIF-1α signaling through siderophore secretion. Additionally, it highlights the significance of the Gut-PHD2-HIF-1α axis in the pathophysiology of diseases associated with ischemia and colitis. By elucidating how siderophores regulate PHD2 at a structural level, this study opens new avenues for utilizing siderophores and their analogs as potential PHD2 inhibitors in ischemic and colitis conditions. This could pave the way for innovative therapeutic strategies aimed at enhancing HIF stabilization through various gut axes, including gut-brain, gut-kidney, and gut-lung interactions. Such approaches have the potential to improve cellular responses to hypoxic stress and offer promising treatments for ischemic injuries and related conditions.

Conclusion

This study elucidates the molecular interactions between gut-derived siderophores and PHD2, providing valuable insights into HIF-1α signaling regulation. By demonstrating the stability and dynamics of these interactions, as well as the energy profiles of the protein–ligand complexes, we addressed the understanding of how gut microbiota influence HIF-1α through siderophore secretion. Our findings underscore the importance of the Gut-PHD2-HIF-1α axis in modulating diseases related to ischemia and colitis, revealing how siderophores regulate PHD2 at the structural level. This study not only opens new avenues for developing siderophore-based inhibitors for PHD2 in ischemic and colitis conditions but also highlights the potential of targeting various gut axes, such as gut-brain, gut-kidney, and gut-lung interactions. Such strategies could enhance HIF stabilization and improve cellular responses to hypoxic stress, offering promising therapeutic approaches for ischemic injuries and related disorders.

Data availability

All data generated or analysed during this study are included in this manuscript.

Received: 9 August 2024; Accepted: 17 December 2024
Published online: 07 January 2025

References

1. Majmundar, A. J., Wong, W. J. & Simon, M. C. Hypoxia-inducible factors and the response to hypoxic stress. *Mol. Cell* **40**, 294–309 (2010).
2. Weidemann, A. & Johnson, R. S. Biology of HIF-1a. *Cell Death Differ.* **15**, 621–627 (2008).
3. Luo, Z. et al. Hypoxia signaling in human health and diseases: Implications and prospects for therapeutics. *Sig. Transduct. Target Ther.* **7**, 218 (2022).
4. McDonough, M. A. et al. Cellular oxygen sensing: Crystal structure of hypoxia-inducible factor prolyl hydroxylase (PHD2). *Proc. Natl. Acad. Sci. U. S. A.* **103**, 9814–9819 (2006).
5. Semenza, G. L. Oxygen sensing, hypoxia-inducible factors, and disease pathophysiology. *Annu. Rev. Pathol.* **9**, 47–71 (2014).
6. Groulx, I. & Lee, S. Oxygen-dependent ubiquitination and degradation of hypoxia-inducible factor requires nuclear-cytoplasmic trafficking of the von Hippel-Lindau tumor suppressor protein. *Mol. Cell Biol.* **22**, 5319–5336 (2002).
7. Zhao, Y. et al. Hypoxia-induced signaling in the cardiovascular system: Pathogenesis and therapeutic targets. *Sig. Transduct. Target Ther.* **8**, 431 (2023).

8. Berra, E., Roux, D., Richard, D. E. & Pouysségur, J. Hypoxia-inducible factor-1α (HIF-1α) escapes O(2)-driven proteasomal degradation irrespective of its subcellular localization: Nucleus or cytoplasm. *EMBO Rep.* **2**, 615–620 (2001).
9. Eckardt, K.-U. et al. Safety and efficacy of vadadustat for Anemia in patients undergoing dialysis. *N. Engl. J. Med.* **384**, 1601–1612 (2021).
10. Dhillon, S. Roxadustat: First global approval. *Drugs* **79**, 563–572 (2019).
11. Semenza, G. L. HIF-1: Mediator of physiological and pathophysiological responses to hypoxia. *J. Appl. Physiol.* **88**, 1474 (2000).
12. Rajendran, G. et al. Inhibition of endothelial PHD2 suppresses post-ischemic kidney inflammation through hypoxia-inducible factor-1. *JASN* **31**, 501–516 (2020).
13. Semenza, G. L. Hypoxia-inducible factors in physiology and medicine. *Cell* **148**, 399–408 (2012).
14. Avivi, A., Resnick, M. B., Nevo, E., Joel, A. & Levy, A. P. Adaptive hypoxic tolerance in the subterranean mole rat Spalax ehrenbergi: The role of vascular endothelial growth factor. *FEBS Lett.* **452**, 133–140.
15. Poyya, J., Joshi, C. G., Kumar, D. J. & Nagendra, H. Sequence analysis and phylogenetic studies of hypoxia-inducible factor-1α. *Cancer Inform.* **16**, 117693511771224 (2017).
16. Leite de Oliveira, R. et al. Gene-targeting of Phd2 improves tumor response to chemotherapy and prevents side-toxicity. *Cancer Cell* **22**, 263–277 (2012).
17. Suhara, T. et al. Inhibition of the oxygen sensor PHD2 in the liver improves survival in lactic acidosis by activating the Cori cycle. *Proc. Natl. Acad. Sci. USA* **112**, 11642–11647 (2015).
18. Flagg, S. C., Martin, C. B., Taabazuing, C. Y., Holmes, B. E. & Knapp, M. J. Screening chelating inhibitors of HIF-prolyl hydroxylase domain 2 (PHD2) and factor inhibiting HIF (FIH). *J. Inorgan. Biochem.* **113**, 25–30 (2012).
19. Abboud, M. I. et al. 2-Oxoglutarate regulates binding of hydroxylated hypoxia-inducible factor to prolyl hydroxylase domain 2. *Chem. Commun. (Camb.)* **54**, 3130–3133 (2018).
20. Foulks, J. M. et al. PAF-acetylhydrolase expressed during megakaryocyte differentiation inactivates PAF-like lipids. *Blood* **113**, 6699–6706 (2009).
21. DeSai, C. & Hays Shapshak, A. *Cerebral Ischemia* (StatPearls StatPearls Publishing, 2022).
22. Speer, R. E. et al. Hypoxia-inducible factor prolyl hydroxylases as targets for neuroprotection by "antioxidant" metal chelators: From ferroptosis to stroke. *Free Radic. Biol. Med.* **62**, 26–36 (2013).
23. Ellermann, M. & Arthur, J. C. Siderophore-mediated iron acquisition and modulation of host-bacterial interactions. *Free Radic. Biol. Med.* **105**, 68–78 (2017).
24. Khasheii, B., Mahmoodi, P. & Mohammadzadeh, A. Siderophores: Importance in bacterial pathogenesis and applications in medicine and industry. *Microbiol. Res.* **250**, 126790 (2021).
25. Siegert, I. et al. Ferritin-mediated iron sequestration stabilizes hypoxia-inducible factor-1α upon LPS activation in the presence of ample oxygen. *Cell Rep.* **13**, 2048–2055 (2015).
26. Dev, S. et al. Role of extracellular hydrogen peroxide in regulation of iron homeostasis genes in neuronal cells: Implication in iron accumulation. *Free Radic. Biol. Med.* **86**, 78–89 (2015).
27. Minervini, G., Quaglia, F. & Tosatto, S. C. E. Insights into the proline hydroxylase (PHD) family, molecular evolution and its impact on human health. *Biochimie* **116**, 114–124 (2015).
28. Liu, W. et al. The signaling pathway of hypoxia inducible factor in regulating gut homeostasis. *Front. Microbiol.* **14**, 1289102 (2023).
29. Tambuwala, M. M. et al. Loss of prolyl hydroxylase-1 protects against colitis through reduced epithelial cell apoptosis and increased barrier function. *Gastroenterology* **139**, 2093–2101 (2010).
30. Bakshi, H. A. et al. Dynamics of prolyl hydroxylases levels during disease progression in experimental colitis. *Inflammation* **42**, 2032–2036 (2019).
31. Berman, H. M. The protein data bank. *Nucleic Acids Res.* **28**, 235–242 (2000).
32. Harder, E. et al. OPLS3: A force field providing broad coverage of drug-like small molecules and proteins. *J. Chem. Theory Comput.* **12**, 281–296 (2016).
33. Friesner, R. A. et al. Extra precision glide: docking and scoring incorporating a model of hydrophobic enclosure for protein−ligand complexes. *J. Med. Chem.* **49**, 6177–6196 (2006).
34. Halgren, T. A. et al. Glide: A new approach for rapid, accurate docking and scoring. 2. Enrichment factors in database screening. *J. Med. Chem.* **47**, 1750–1759 (2004).
35. Godschalk, F., Genheden, S., Söderhjelm, P. & Ryde, U. Comparison of MM/GBSA calculations based on explicit and implicit solvent simulations. *Phys. Chem. Chem. Phys.* **15**, 7731 (2013).
36. Hou, T., Wang, J., Li, Y. & Wang, W. Assessing the performance of the molecular mechanics/Poisson Boltzmann surface area and molecular mechanics/generalized Born surface area methods. II. The accuracy of ranking poses generated from docking. *J. Comput. Chem.* **32**, 866–877 (2011).
37. Poyya, J., Kumar, D. J., Nagendra, H. G., Dinesh, B., Aditya Rao, S. J. & Joshi, C. G. (2021). Receptor based virtual screening of potential novel inhibitors of tigar [TP53 (tumour protein 53)-induced glycolysis and apoptosis regulator. *Med. Hypoth.* 110683.
38. Shi, M. et al. Inhibition mechanism of hydroxyproline-like small inhibitors to disorder HIF-VHL interaction by molecular dynamic simulations and binding free energy calculations. *Chin. J. Chem. Phys.* **34**, 814–824 (2021).
39. Poyya, J., Danagoudar, A., Joshi, C. G., Khandagale, A. S. & Narayanappa Govinda, R. Computational investigation of endophytic fungal (penicillium citrinumCGJ-C2) compound and its in-silico derivatives for the inhibition of RNA-dependent RNA polymerase of SARS-CoV-2. *COVID* **4**, e161023222258 (2023).
40. Fong, G.-H. & Takeda, K. Role and regulation of prolyl hydroxylase domain proteins. *Cell Death Differ.* **15**, 635–641 (2008).
41. Poon, E., Harris, A. L. & Ashcroft. M. Targeting the hypoxia-inducible factor (HIF) pathway in cancer. *Expert Rev. Mol. Med.* **11**, null-null (2009).
42. Liang, Z. & Li, Q. X. π-cation interactions in molecular recognition: Perspectives on pharmaceuticals and pesticides. *J. Agric. Food Chem.* **66**, 3315–3323 (2018).
43. Bissantz, C., Kuhn, B. & Stahl, M. A medicinal chemist's guide to molecular interactions. *J. Med. Chem.* **53**, 5061–5084 (2010).
44. Chowdhury, R. et al. Selective small molecule probes for the hypoxia inducible factor (HIF) prolyl hydroxylases. *ACS Chem. Biol.* **8**, 1488–1496 (2013).
45. Flanigan, W. R. & Jain, I. H. The goldilocks oxygen principle: Not too little and not too much. *Nat. Cardiovasc. Res.* **1**, 1101–1103 (2022).
46. Kalogeris, T., Baines, C. P., Krenz, M. & Korthuis, R. J. Cell Biology of Ischemia/Reperfusion Injury. In *International Review of Cell and Molecular Biology* 229–317. (Elsevier, 2012).
47. Loor, G. & Schumacker, P. T. Role of hypoxia-inducible factor in cell survival during myocardial ischemia–reperfusion. *Cell Death Differ.* **15**, 686–690 (2008).
48. Conde, E. et al. HIF-1α induction during reperfusion avoids maladaptive repair after renal ischemia/reperfusion involving miR127-3p. *Sci. Rep.* **7**, 41099 (2017).
49. Mohsen, Y. et al. The different types of metallophores produced by salmonella enterica: A review. *Microbiol. Res.* **14**, 1457–1469 (2023).
50. Winterbourn, C. C., Kettle, A. J. & Hampton, M. B. Reactive oxygen species and neutrophil function. *Annu. Rev. Biochem.* **85**, 765–792 (2016).
51. Hou, K. et al. Microbiota in health and diseases. *Sig. Transduct. Target. Ther.* **7**, 135 (2022).

52. Rolhion, N. & Chassaing, B. When pathogenic bacteria meet the intestinal microbiota. *Philos. Trans. R. Soc. Lond. B Biol. Sci.* **371**, 20150504 (2016).
53. Saha, P. et al. Enterobactin, an iron chelating bacterial siderophore, arrests cancer cell proliferation. *Biochem. Pharmacol.* **168**, 71–81 (2019).
54. Gokarn, K., Sarangdhar, V. & Pal, R. B. Effect of microbial siderophores on mammalian non-malignant and malignant cell lines. *BMC Complement Altern. Med.* **17**, 145 (2017).
55. Chowdhury, R. et al. Structural basis for oxygen degradation domain selectivity of the HIF prolyl hydroxylases. *Nat. Commun.* **7**, 12673 (2016).

Acknowledgements
The author expresses gratitude to Google Inc. for generously providing Google Research Cloud Credit (EDU Credit—wilsonjessica—209474439) and to the SDM Research Institute for Biomedical Sciences and Shri Dharmasthala Manjunatheshwara University, and Department of Biochemistry and Industrial Chemistry, Mangalore University for their facility.

Author contributions
JIP: Methodology, JP: Conceptualization, Methodology, writing-review and editing, project administration, supervision, and editing manuscript, NK: Visualization, AP: Visualization, English editing, ASK: J: Review, CGJ: Review and Editing, SRK: Review and Editing, KS: J: Review and Editing.

Competing interests
The authors declare no competing interests.

Additional information
Supplementary Information The online version contains supplementary material available at https://doi.org/10.1038/s41598-024-83730-8.

Correspondence and requests for materials should be addressed to J.P.

Reprints and permissions information is available at www.nature.com/reprints.

Publisher's note Springer Nature remains neutral with regard to jurisdictional claims in published maps and institutional affiliations.